Available online at www.sciencedirect.com
SCIENCE DIRECT®
Journal of the European Ceramic Society 25 (2005) 393–400
www.elsevier.com/locate/jeurceramsoc

Studies of the sintering kinetics of thick thermal barrier coatings by thermal diffusivity measurements

F. Cernuschi [a,*], L. Lorenzoni [a], S. Ahmaniemi [b,1], P. Vuoristo [b], T. Mäntylä [b]

[a] *CESI S.p.a., Via Reggio Emilia, 39, 20090 Segrate (MI), Italy*
[b] *Tampere University of Technology, Institute of Materials Science, P.O. Box 589, 33101 Tampere, Finland*

Received 24 October 2003; received in revised form 19 January 2004; accepted 25 January 2004
Available online 2 June 2004

Abstract

Better thermal insulation of the hot path components is needed in state-of-the-art gas turbines and diesel engines, because of the increasing demands of the higher process temperatures. In these processes, thermal barrier coatings (TBCs) and various cooling techniques mainly control the component surface temperatures. For this reason low thermal conductivity of the TBCs are extensively studied. One of the main factors determining the TBC thermal conductivity is the coating microstructure, with specific attention to the porosity content, as well as to its morphology and orientation. One important feature of TBCs is the stability of their thermal properties as a function of time at service conditions. In fact the prolonged exposure to high temperature can promote shrinkage phenomena within the TBC, which make the coating less strain tolerant and more heat conductive. This leads to a drastic reduction of the functional effectiveness of this ceramic protective top layer.

In order to study the evolution of thermal properties of TBC, as a function of time and temperature, thermal diffusivity evaluation by laser flash method has been performed. The measurements have been performed on freestanding yttria-stabilized zirconium oxide (YPSZ) TBCs. In particular, measurements have been carried out at five different temperatures in the range 900–1300 °C, for different ageing times (from 1 up to 150 h). The data show a significant increase of the thermal diffusivity also after exposures of few hours, especially at the highest testing temperatures. Microstructural analysis carried out by optical and electron microscopy clearly showed that the observed thermal diffusivity variations can be ascribed to sub-micrometric crack healing and sintering neck formation. Mechanical testing confirmed the microhardness increase of TBC as well. Finally the data have been summarised in order to experimentally define a "functional life" curve of the TBC, as a function of ageing time and temperature.

Keywords: Porosity; Thermal conductivity; ZrO_2; Plasma spraying; Sintering; Thermal barrier coatings

1. Introduction

Ceramic thermal barrier coatings (TBCs) are widely applied in last generation gas turbines hot path components. In particular vanes, blades, transition pieces and combustion chambers are protected from hot gases by depositing on their surfaces a refractory ceramic porous layer. The state-of the-art of these TBC is represented by yttrium oxide partially stabilised zirconium oxide (7–8 wt.%Y_2O_3 + ZrO_2) deposited onto the components either by air plasma spray (APS) or by electron beam-physical vapour deposition (EB-PVD).[1–3] In particular, due to the deposition process, the microstructure of APS coatings results to be the superposition of fused splats of yttria-stabilized zirconium oxide (YPSZ). Thus, the porosity consists of inter-splat spherical porosity and inter-, intra- and trans-lamellar microcracks with the smaller axis typically oriented parallel (inter-lamellae) and perpendicular (intra- and trans-lamellae) to the heat flux (i.e. through-the-thickness of the TBC).[4–8] EB-PVD coatings have the typical columnar structure oriented in parallel to the heat flux. The porosity of these coatings has a bimodal distribution constituted mainly by the space between the columns of TBC (even well represented by columns) and by intra-columnar micropores.[9,10]

It is well known that this difference in microstructure between APS and EB-PVD, as well as the difference between

* Corresponding author. Tel.: +39-022-125-4577; fax: +39-022-125-4678.
E-mail address: cernuschi@cesi.it (F. Cernuschi).
[1] Currently at Metso Paper Inc., Global Service Operations, P.O. Box 587, FIN-40101 Jyväskylä, Finland.

0955-2219/$ – see front matter © 2004 Published by Elsevier Ltd.
doi:10.1016/j.jeurceramsoc.2004.01.009

APS coatings produced by using different process parameters, can affect the strain tolerance, the elastic modulus, the thermal conductivity, the erosion resistance and the sintering activity of TBC.

As far as sintering activity is concerned, the key factors discriminating coatings with different microstructures are the content, the shape and the size of either pores or microcracks and the presence of low melting temperature impurities (typically silica) within the TBC.[5–9,11–14] Sintering phenomena of TBCs depend also on boundary conditions of the coating (i.e. free-standing or adherent to a metallic substrate) and on the presence of a thermal gradient through-the-thickness during the ageing. In fact, the thermal expansion mismatch caused by the two aforementioned conditions can promote the nucleation and the opening of crack close to the TBC surface thus opposing to the sintering activity.

Previous studies describe the sintering of TBC as consisting of two separate phases. The first, mainly active at very short times (<10 h), is characterised by the improvement of the inter-splat bonding produced by healing microcracks and by the trans-splat grain growth and in the reduction of intra-columnar micropores in APS and EB-PVD coatings, respectively. The latter sintering quasi-stationary stage promotes mainly pore shape changes (making the aspect ratio of the flat spheroid tend to values close to that of spheres), the reduction of macro-pore volumes and the "welding" of neighbouring columns in APS and EB-PVD coatings, respectively.[5–7,9,12,13] In particular, phenomena involved in microcrack healing and shape changes are reported to take place at temperatures as low as 900 °C, while the pore system seems to be affected by sintering only at temperatures higher than 1200–1300 °C.[5,7]

Sintering modifies the mechanical and thermo-physical properties of TBC. In particular, the microhardness and the elastic modulus strongly increase with sintering reducing the strain compliance and thus the "life" of the TBC. In fact, the healing of microcracks, as well as the formation of bridges between splats, promote chemical bondings. The drawback of the formation of these bondings is that a crack is allowed to propagate through different grains without being deflected.

Moreover, crack healing and modifications of the aspect ratio of pores both contribute to increase significantly the thermal conductivity of the TBC which is no more effective in the protection of the bulk metallic material from overheating.

Thus, the study of the sintering kinetic as a function of the ageing time and temperature is essential for selecting the TBC with the best long term performances.

In this work, the results of a preliminary activity devoted to characterise the sintering kinetic of APS TBC by measuring the microhardness and the thermal diffusivity $\alpha = k/\rho C$ (where k, C and ρ are the thermal conductivity, the specific heat and the volumic mass, respectively) are reported. The two final aims of this research activity are to obtain "life curves" for TBCs produced by using different zirconia powders and spraying process parameters and to set-up a NDE technique able to monitor the evolution of sintering directly on serviced components during maintenance stops, in order to prevent the TBC spallation.

Table 1
Sample thickness as measured by image analysis

Sample	T1	T2	T3	T4	T45
Thickness (μm)	966.88	958.25	980.3	995.95	982.75
Standard deviation (μm)	26.75	36.21	31.82	30.67	34.09

2. Experimental

2.1. The samples

For this experimental activity, six thick YPSZ samples (named T1–T6) deposited by APS have been used. The TBCs have been detached from the metallic substrates by chemical etching. Then, from each sample, a 10 mm diameter disk shape free standing TBC specimen have been extracted for thermal diffusivity measurements. Table 1 resumes the specimen coating thickness, as measured by image analysis along the section of the remaining ring shape TBC samples.

2.2. Measurement technique

Thermal diffusivity measurements have been carried out by using the laser flash technique.[15,16] This method consists of heating the front face of a sample (typically a small disk-shaped specimen) by a short laser pulse and detecting the temperature rise on its rear surface by an infrared detector. For evaluating the thermal diffusivity a, the solution proposed originally by Parker et al.[15] consisted of using the following relation

$$\alpha = 0.1388\frac{L^2}{t_{1/2}} \tag{3}$$

where $t_{1/2}$ and L are the time corresponding to the half-maximum increase of the temperature and the sample thickness. The main advantages of this method are the simplicity and rapidity of measurement, and the possibility to measure the thermal diffusivity on a wide range of materials within a wide temperature range.

The experimental system consists of a pulsed 1.06×10^{-6} m wavelength Nd:YAG laser (Laser Metrics, Winterpark, FL, USA) as the heating source. The laser beam shape is circular with a uniform intensity. The sample is located within a tantalum furnace with a molybdenum shield (Theta Instruments, Port Washington, NY, USA) where it is possible to reach 1500 °C. The sample and the furnace are both inside a vacuum chamber, and an infrared detector can detect, without any contact, the temperature of the rear face of

the sample through an infrared window. The signal is then amplified, acquired and processed by a PC.

As YPSZ is translucent in the near infrared, in order to make the surfaces opaque for guaranteeing the absorption and the detection of the IR radiation just on the sample surfaces, prior performing the thermal diffusivity measurement, on both the front and the rear faces of the sample, a thin layer of colloidal graphite was painted following a procedure described and discussed elsewhere.[17]

Since measurements have been carried out in vacuum, the only correction applied to the experimental data was related to the radiative losses taking place at high temperature. In this specific case, the Cowan method for reducing the data has been used.[16,18]

2.3. Experimental procedure

The procedure followed to monitor the sintering process of TBC consisted in the following steps:

- Measuring the thermal diffusivity of T1–T5 samples at 200 °C by Laser Flash (L.F.) technique.
- Heating up the samples to the ageing (and measurement) temperature that was fixed for the five samples equal to 900, 1000, 1100, 1200 and 1300 °C, respectively.
- When reached the fixed temperature, the first L.F. measurement was carried out (time 0). Subsequent L.F. measurements were performed always maintaining the sample at the ageing temperature. For each sample, data have been collected at different times in the interval 0–150 h and at each time, five consecutive measurements were carried out for statistical reasons.
- During the cooling stage at the end of the experiment, thermal diffusivity at 200 °C was measured again on the aged samples.

After these measurements, microhardness measurements have been carried out on the five aged samples (T1–T5) and on the as-sprayed one (T6).

2.4. The experimental results

For each sample, Fig. 1 shows the thermal diffusivity as a function of the ageing time. In order to compare the experimental data referring to different ageing temperatures, making more evident for each sample the relative thermal diffusivity increase (caused by the sintering phenomena), the normalisation of the experimental values in respect to the first measured value (i.e. that get at the time 0) has been carried out. Fig. 2 summarises the results of this normalisation. Since normalising eliminate the uncertainty related to the TBC thickness evaluation, this approach could be useful for practical applications when the thermal diffusivity measurement is carried out directly on real components using single side photothermal and/or thermographic techniques.

For all the samples, two sintering phases can be clearly discriminated in Figs. 1 and 2. In fact, at first, within few ageing hours (<10 h) a significant increase of thermal diffusivity can be observed at each temperature followed by a slower rate sintering activity. For the three lower ageing temperatures (900, 1000 and 1100 °C) data seem to tend asymptotically to values below 1.15 while the sintering rate at 1200 and 1300 °C does not show evident upper limits and exhibits higher slopes. This can be explained taking into

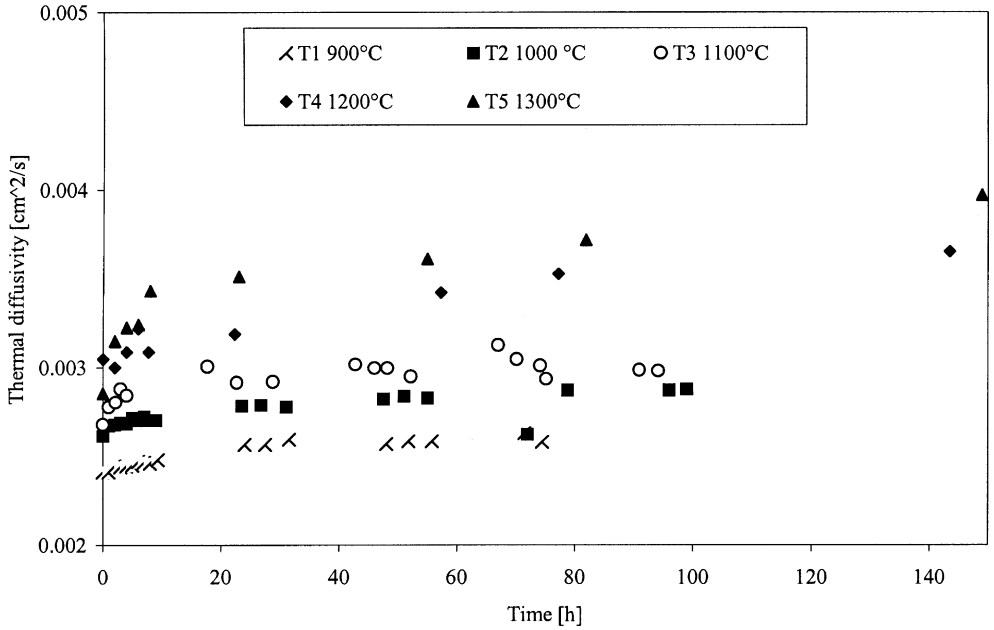

Fig. 1. Thermal diffusivity vs. time for ageing temperature equal to (⅄) 900°C, (■) 1000 °C, (○) 1100 °C, (◆) 1200 °C and (▲)1300 °C, respectively.

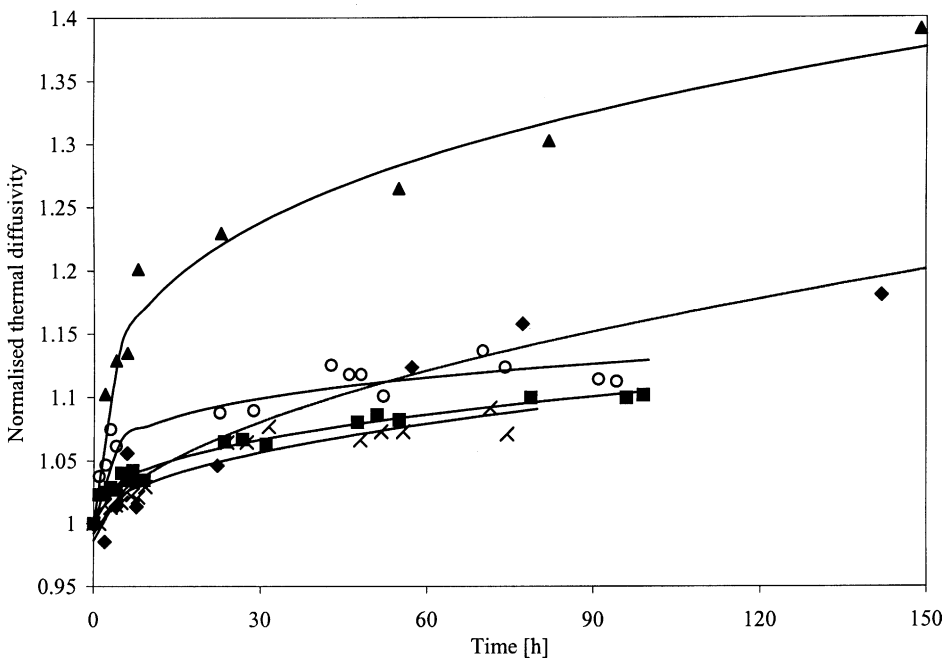

Fig. 2. Normalised thermal diffusivity vs. ageing time for ageing temperature equal to (⅄) 900°C, (■) 1000 °C, (○) 1100 °C, (◆) 1200 °C and (▲)1300 °C, respectively. The solid lines represent the best fitting of the experimental data measured at the five ageing temperatures.

account that the stationary sintering phase is active at temperatures higher than 1200 °C.[5,7]

The comparison between absolute values of thermal diffusivity of the five samples can be carried out on the thermal diffusivity values measured at 200 °C both before and after ageing as shown in Table 2. The increase of thermal diffusivity measured at 200 °C caused by the sintering phenomena affects differently the samples as a function of ageing temperature and time. In fact, sample T1 and T5, aged at 900 and 1300 °C, respectively, exhibit a very small (7.3%) and very large (94.3%) increase of thermal diffusivity. For each sample, the different thermal diffusivity increase observed at low (200 °C) and at high (ageing) temperatures can be explained taking into account that the radiative contribution to the heat transport within the TBC is negligible at low temperatures but is significant at ageing temperatures.

In order to discriminate between the effects related to sintering phenomena, chemical reactions, partial evaporation, and phase transformations, supplementary analyses have been performed. In particular, on an as sprayed sample, the specific heat C_p in argon atmosphere has been evaluated in the range 100–1300 °C, by using a differential scanning calorimeter DSC 404 C (Netzsch-Geratebau GmbH, Selb, Germany). Three consecutive measurement cycles have been carried out to discriminate between reversible and not reversible reactions. From the experimental data shown in Fig. 3, it results that no relevant chemical reaction took place, apart from an exothermic irreversible reaction at about 800 °C observed during the first cycle, probably caused by residual stress relaxation. Furthermore, the X-ray diffraction analysis carried out on the six T1–T6 samples after the high temperature exposure, using a D500 X-ray diffractometer (Siemens, Karlsruhe, Germany), confirms that no phase transformation took place during the high temperature exposure as shown by Fig. 4. The C_p and XRD results indicate that sintering phenomena are the principal cause of the thermal diffusivity increase during the ageing period.

At last, samples have been cut and, after the surface polishing, the hardness on the section was measured by Vickers indentation using a weight of 300 g. In order to improve the statistic, for each sample, 10 measurements have

Table 2
Thermal diffusivity at 200 °C

Sample	Ageing time (h)	Ageing temperature (°C)	Thermal diffusivity before ageing (cm^2/s)	Thermal diffusivity after ageing (cm^2/s)	Relative thermal diffusivity increase (%)
T1	94	900	0.00300	0.00322	7.3
T2	99	1000	0.00287	0.00369	28.6
T3	94	1100	0.00283	0.00397	40.3
T4	142	1200	0.00296	0.00481	62.5
T5	149	1300	0.00283	0.0055	94.3

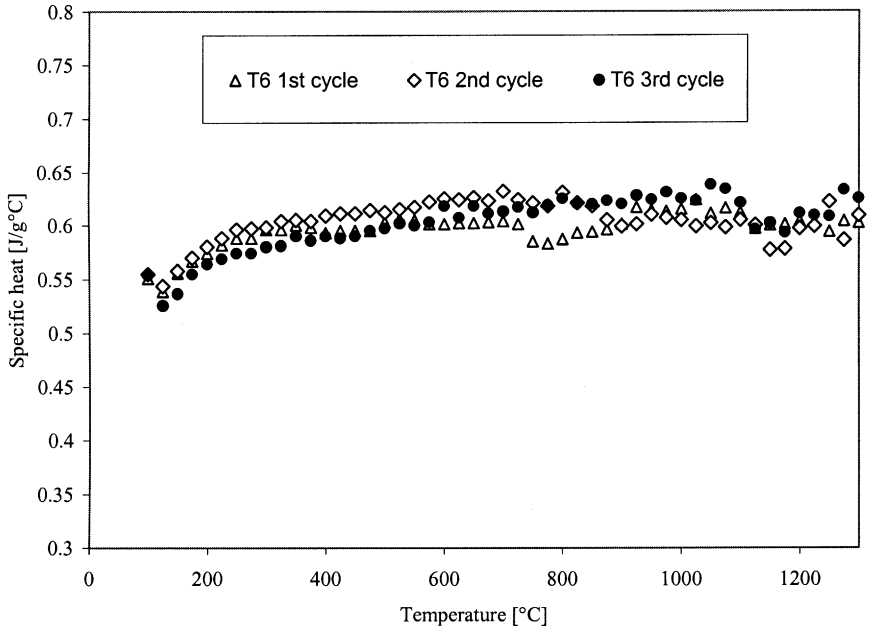

Fig. 3. Specific heat C_p as a function of the temperature for the sample T6. Three consecutive measurement cycles have been performed in order to distinguish between reversible and irreversible transformations. Measurements have been carried out in Argon inert atmosphere.

been carried out. Fig. 5 clearly shows a correlation between the hardness increase and the ageing temperature due to sintering phenomena.

Since the final aim of this activity is to define experimentally a curve correlating the normalised thermal diffusivity versus the TBC "life", the first step consists in reducing to a 2D-representation the natural 3D-representation of the dependence of TBC thermal diffusivity from ageing temperature T and time t by combining together these two parameters using the well know Larson–Miller parameter (LMP), defined as follows

$$\mathrm{LMP} = T(\ln(t+1)+20) \quad (1)$$

where temperature and time should be expressed in Kelvin and hours, respectively. Notwithstanding the use of the LMP is generally used in the creep–rupture analysis, its application in this field can be considered because experimental data indicate that the effect of time and temperature on the thermal diffusivity increase can be quite well represented by logarithmic and linear functions, respectively. Fig. 6 summarises semi-logarithmically all the experimental data

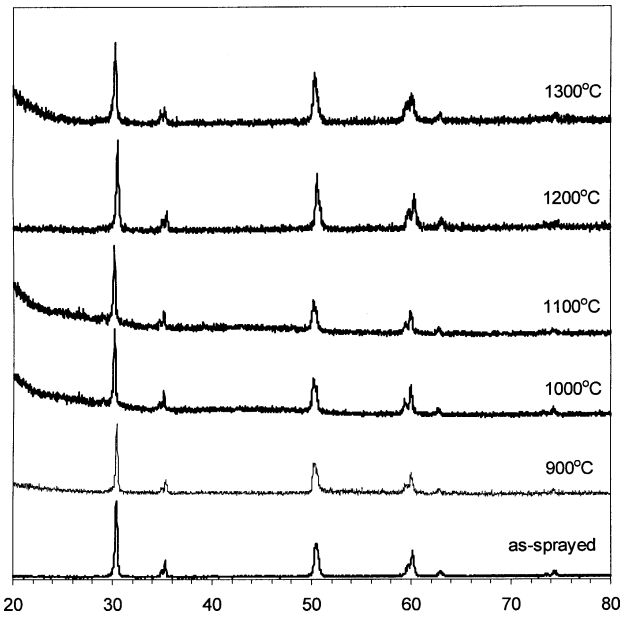

Fig. 4. X-ray diffraction spectra for the six samples T1–T6. Measurements have been carried out after the ageing at high temperature using the Cu Kα radiation. The scanning step was fixed equal to 0.02° with a scan rate of three steps per second.

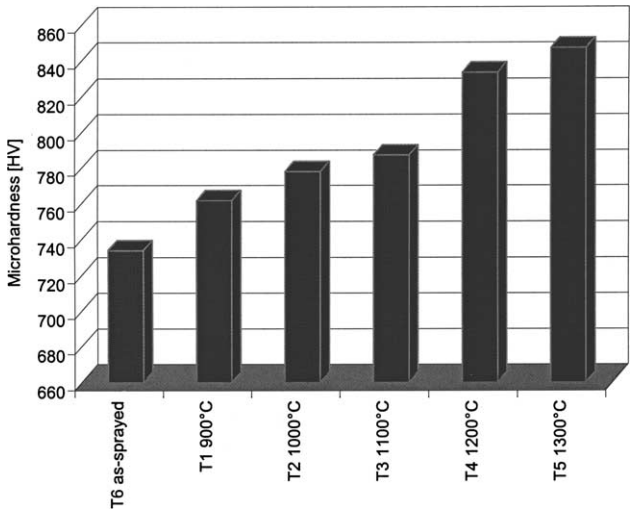

Fig. 5. Vickers microhardness of samples T1–T6. For each sample, values refer to the average of 10 measurements carried out along the section.

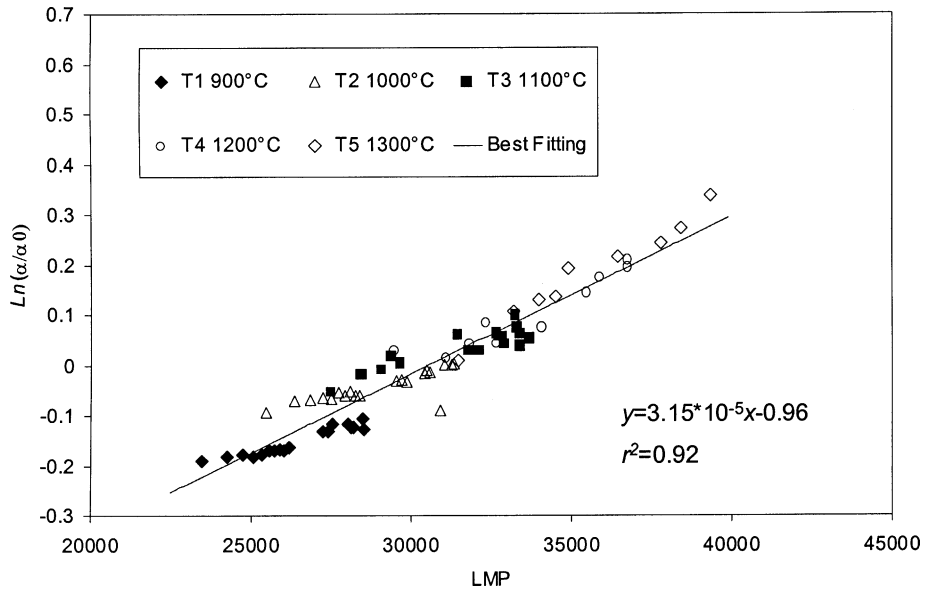

Fig. 6. Natural logarithm of the normalised thermal diffusivity at ageing temperatures vs. LMP for samples T1–T5.

using LMP. In particular, for each sample, thermal diffusivity values measured at the ageing temperature have been normalised by the corresponding value measured at 200 °C before heating up the sample.

3. Discussion

As the density and specific heat variations due to ageing usually are almost negligible if compared with the corresponding modification of thermal conductivity, the relative increase of thermal conductivity and diffusivity values can be compared without any further computation.[19,20] In particular, the results of this preliminary work on the sintering kinetics of 7–8 wt.% $Y_2O_3 + ZrO_2$ APS free standing coatings (aged in vacuum and measured by a transient technique) show a good agreement with the corresponding values reported in the literature, notwithstanding those data refer to thermal conductivity variations as measured in air on three layers samples (TBC-bondcoat-base metal) by a laser steady-state heat flux method.[13,21] The relative increase of the thermal diffusivity aged at the different temperatures shown in Fig. 2 results smaller than those reported by Zhu and Miller[13,21] for APS TBC samples aged at 990, 1100 and 1320 °C in the first 30 ageing hours. In particular, they report an increase of 8, 15 and 45% for samples aged at 990, 1100 and 1320 °C, respectively, while in the present work after 30 h an increase of 6, 9 and 25%, respectively, are observed. This difference can be mainly ascribed to the fact that these literature results have not been normalised to the initial value. Thus, for each TBC sample, the reported absolute value of thermal diffusivity consists of the superimposition of the effects of sintering phenomena taking place at high temperature to the initial value of thermal diffusivity at the measurement temperature, which differs from sample to sample. On the contrary, normalising the experimental data, as done in Fig. 2, the pure effects produced by sintering on the thermal diffusivity of TBCs can be better highlighted.

As far as the absolute thermal diffusivity values of thick TBCs are concerned, a good agreement with literature is found. In particular, as far as low temperature (i.e. 200 °C) measurements are concerned, before heating, the average value for T1–T5 samples is 0.00289 cm^2/s that is in good agreement with the thermal diffusivity value of 0.0032 cm/s at 200 °C reported by Wang and Dinwiddie[22] for an APS YPSZ TBC. In the literature are reported thermal diffusivity values at low temperatures specifically referred to thick TBC, in the ranges 0.0033–0.0042 cm^2/s[20] and 0.002–0.0055 cm^2/s, depending to the peculiar microstructure of the coatings.[23] Concerning the increase of thermal diffusivity after heat treatments, Schwingel et al.[23] report an increase of about 22% of the thermal diffusivity, as measured at 100 °C after an exposure at 1200 °C for few hours. For the sample T4 (aged at 1200 °C for 142 h), an increase of 62% has been observed. Bianchi et al. and Dutton et al. report an increase of about 33 and 46% of the thermal diffusivity as measured at 200 °C after an exposure at 1300 °C for few (<3) and 50 h, respectively.[6,20] The corresponding result within this work shows a relative increase of 94% for the sample T5 (aged at 1300 °C for 149 h).

Clearly, for each ageing temperature, the difference between all these results depends mainly from the time of exposure at the high temperature.

In general, when comparisons between literature data are carried out, it must be taken into consideration that thermal diffusivity values of porous samples measured in vacuum usually result lower than values obtained in inert atmosphere because the gas filling pores contributes to the heat transfer.

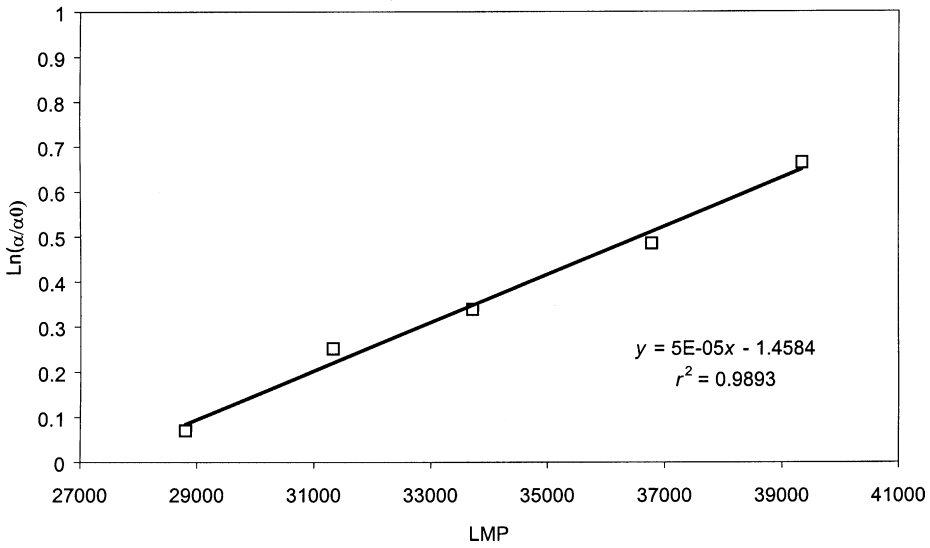

Fig. 7. Natural logarithm of the normalised thermal diffusivity at 200 °C vs. LMP for samples T1–T5.

Moreover, a more complex situation has to be faced when measurements are carried out in air because some chemical reactions could take place. Furthermore, the bonding of the TBC to a metallic substrate, having typically a higher thermal expansion coefficient than the TBC itself, partially prevents the microcrack healing and could also promote cracks formation, as well as the through-the thickness heat gradient does.

By analysing the laser flash experimental data, small fluctuations of thermal diffusivity values can be observed. A possible explanation of this phenomenon is that the heating pulse impinging on the front face of the sample can cause almost instantaneously a through-the-thickness differential thermal expansion which can prevent the healing or even promote the nucleation of micro cracks inside the TBC. In order to minimise the effects of the laser pulse on the measured thermal diffusivity values, a reduction of both the laser energy and the number of measures is suggested.

The measurement strategy followed for this preliminary study allowed to minimise the number of both TBC samples and operations, but when data referring to different ageing temperatures are combined together as in Fig. 6, a fictitious contribution, due to the fact that thermal diffusivity values refer to measurements carried out at different temperatures, is superimposed to the true trend of thermal diffusivity versus LMP. This drawback can be avoided by analysing thermal diffusivity measurements carried out at 200 °C both before and after ageing as shown in Fig. 7. However, for future activities, testing procedure could consists in ageing samples at different temperatures,[3] but measuring the thermal diffusivity at a fixed temperature equal for all the samples (for example fixed equal to 1100 °C). Nevertheless, following this approach, it should be taken into account that samples aged at either lower or higher temperatures will be subjected to a thermal cycling each time a thermal diffusivity measurement will be carried out. On the other hand, different measurement approaches would require increasing the number of samples and the detrimental sample handling and positioning.

Although the trend of the thermal diffusivity values is not perfectly the same for the five TBCs samples, such a representation can help in obtaining worthy indications for estimating the residual life of TBC. Since the slopes of data referring to the low ageing temperatures (900 and 1100 °C) slightly differ from those referring to high ageing temperatures (1200–1300 °C), in order to obtain conservative estimation of the residual life, a weighted fitting of the experimental data, if necessary, could be suggested (if the slope difference would be still present also after having eliminated the fictitious contribution previously described).

Since the final aim is to monitor, directly on coated components, the thermal diffusivity evolution of TBC as a parameter accounting for sintering phenomena, the curve α/α_0 versus LMP should be built also using low temperature measurements (i.e. at RT). Subsequently, a correlation between this curve and the corresponding one at high temperature should also be obtained. One of the techniques suitable to be applied to the RT thermal diffusivity evaluation of TBC deposited onto hot path components such as blades, is thermal waves interferometry (TWI).[24–26] The normalisation of thermal diffusivity data, as performed in this work, is suggested in order to avoid to precisely measure the TBC thickness. In fact, for coated components, Eddy currents systems can be successfully used to measure non destructively the TBC thickness but, due to the contact between the probe and the coating surface, the thickness is differently overestimated as a function of the coating surface roughness. On the contrary, normalising requires only performing thermal diffusivity measurements at the same position of the component surface. This can be guaranteed by fixing the measured area sufficiently wide if compared with uncertainty of the re-positioning process.

Acknowledgements

This study has been conducted within the frame of "Ric rca di Sistema" D. L. MCCA 26/01/2000.

References

1. Swaminathan, V. P. and Cheruvu, N. S., Gas turbine hot-section materials and coatings in electric utility applications. In *Advanced Materials and Coatings for Combustion Turbines*, ed. V. P. Swaminathan and N. S. Cheruvu. ASM International, 1994.
2. Beele, W., Marijnissen, G. and Van Lieshout, A., The evolution of thermal barrier coatings-status and upcoming solutions for today's key issues. *Surf. Coat. Technol.* 1999, **120/121**, 61–67.
3. Nicholls, J. R. and Wing, R., Advances in coating systems for utility gas turbines. In *Proceedings of Materials for Advanced Power Engineering 2002*, ed. J. Lecomte-Beckers, M. Carton, F. Schubert and P. J. Ennis. Schriften des Forschungszentrum, Julich, pp. 449–463.
4. Leigh, S. and Berndt, C. C., Quantitative evaluation of void distributions within a plasma-sprayed ceramic. *J. Am. Ceram. Soc.* 1999, **82**(1), 17–21.
5. Ilavsky, J., Long, G. G., Allen, A. J. and Berndt, C. C., Evolution of the void structure in plasma-sprayed YSZ deposits during heating. *Mater. Sci. Eng.* 1999, **A272**, 215–221.
6. Dutton, R., Wheeler, R., Ravichandran, K. S. and An, K., Effect of heat treatment on the thermal conductivity of plasma-sprayed thermal barrier coatings. *J. Thermal Spray Technol.* 2000, **9**(2), 204.
7. Thompson, J. A. and Clyne, T. W., The effect of heat treatment on the stiffness of zirconia top coats in plasma-sprayed TBCs. *Acta Mater.* 2001, **49**, 1565–1575.
8. McPherson, R., A review of microstructure and properties of plasma sprayed ceramic coatings. *Surf. Coat. Technol.* 1989, **39/40**, 173–181.
9. Zhu, D., Miller, R. A., Nagaraj, B. A. and Bruce, R. W., Thermal conductivity of EB-PVD thermal barrier coatings evaluated by a steady-state laser heat flux technique. *Surf. Coat. Technol.* 2001, **138**, 1–8.
10. Scardi, P., Leoni, M., Cernuschi, F. and Figari, A., Microstructure and heat transfer phenomena in ceramic thermal barrier coatings. *J. Am. Ceram. Soc.* 2001, **84**(4), 827–835.
11. Siebert, B., Vassen, R. and Stoever, D., Changes in porosity and Young's modulus due to sintering of plasma sprayed thermal barrier coatings. *J. Mater. Process. Technol.* 1999, **92/93**, 217–223.
12. Eaton, H. E. R. C., Sintering studied of plasma sprayed zirconia. *Surf. Coat. Technol.* 1987, **32**, 227–236.
13. Zhu, D. and Miller, R. A., Thermal conductivity and elastic modulus evolution of thermal barrier coatings under high heat flux conditions. *J. Thermal Spray Technol.* 2000, **9**(2), 175.
14. Janos, B. Z., Lugscheider, E. and Remer, P., Effect of thermal ageing on the erosion resistance of air plasma sprayed zirconia thermal barrier coating. *Surf. Coat. Technol.* 1999, **113**, 278–285.
15. Parker, W. P., Jenkins, R. J., Butter, C. P., Gutter, G. L. and Abbott, G. L., *J. Appl. Phys.* 1961, **32**, 1679.
16. Taylor, R. E. and Maglic, K. D., *Compendium of Thermophysical Property Measurement Methods, Vol 1: Survey of Measurement Techniques*, ed. K. D. Maglic *et al.* Plenum Press, New York, 1984, pp. 299–333.
17. Cernuschi, F., Lorenzoni, L., Bianchi, P. and Figari, A., The effects of sample surface treatments on laser flash thermal diffusivity measurements. *Infrared Phys. Technol.* 2002, **43**(3–5), 133–138.
18. Cowan, R. D., Pulse method of measuring thermal diffusivity at high temperature. *J. Appl. Phys.* 1963, **34**, 926.
19. Ahmaniemi, S., Vuoristo, P., Mantyla, T., Cernuschi, F. and Lorenzoni, L., Modified thick thermal barrier coatings. Thermophysical characterization. *J. Eur. Ceram. Soc.* 2004, **24**(9), 2669–2679.
20. Bianchi, P., Cernuschi, F., Lorenzoni, L., Ahmaniemi, S., Vippola, M., Vuoristo, P. *et al.*, Thermophysical and microstructural characterisation of modified thick yttria stabilised zirconia thermal barrier coatings. In *Proceedings of Materials for Advanced Power Engineering 2002*, ed. J. Lecomte-Beckers, M. Carton, F. Schubert and P. J. Ennis. Schriften des Forschungszentrum, Julich, pp. 449–463.
21. Zhu, D. and Miller, R. A., *Thermal Conductivity and Elastic Modulus Evolution of Thermal Barrier Coatings under High Heat Flux Conditions.* NASA report NASA/TM-1999-209069, April 1999.
22. Wang, H. and Dinwiddie, R. B., Reliability of laser flash thermal diffusivity measurements of the thermal barrier coatings. *J. Thermal Spray Technol.* 2000, **9**(2), 210.
23. Schwingel, D., Taylor, R., Haubold, T., Wigren, J. and Gualco, C., Mechanical and thermophysical properties of thick PSYZ thermal barrier coatings: correlation with microstructure and spraying parameters. *Surf. Coat. Technol.* 1998, **108/109**, 99–106.
24. Bennet, Jr. C.A. and Patty, R. R., Thermal wave interferometry: a potential application of the photoacoustic effect. *Appl. Opt.* 1982, **21**, 49–54.
25. Almond, D. P. and Patel, P. M., *Photothermal Science and Techniques*. Chapman & Hall, London, 1996.
26. Scardi, P., Leoni, M., Cernuschi, F. and Figari, A., Microstructure and heat transfer phenomena in ceramic thermal barrier coatings. *J. Am. Ceram. Soc.* 2001, **84**(4), 827–835.